

RECOVERY OF USED LUBRICATING OIL BY GLACIAL ACETIC ACID WITH TWO DIFFERENT ACTIVATED CARBONS

S. M. Anisuzzaman^{1,2*} and Mohammad Hafiz Jumaidi²

¹Energy Research Unit (ERU),

²Chemical Engineering Programme, Faculty of Engineering,
Universiti Malaysia Sabah, 88400 Kota Kinabalu, Sabah, Malaysia.

*Corresponding author: anis_zaman@ums.edu.my

Received 23rd June 2022; accepted 11th July 2022

Available online 1st Nov 2022

Doi: <https://doi.org/10.51200/bsj.v43i2.4510>

ABSTRACT: Recovery of used lubricating oil (ULO) generally comprises cleaning, drying, and adsorption in order to eliminate water, sludge, and impurities. As the ULO is one of the hazardous wastes generated in various industrial and automotive industries, it should not be used or disposed of in ways that are harmful to the environment. The main purpose of this study was to investigate the effectiveness of two different types of activated carbons (ACs) which are coconut AC (CAC) and rice husk AC (RHAC) in recovering the ULO. Glacial acetic acid was used in the acid treatment as it does not react with the base oils, and the ACs were substituted with the clay used in the clay treatment. The recovered oil was analysed through analytical characterizations, which are Fourier transform infrared spectroscopy (FTIR), ultraviolet-visible (UV-vis) spectroscopy and atomic absorption spectrometry (AAS). FTIR analysis revealed that the properties of the untreated ULO samples improved by removing the carbonyl compounds. In terms of metal removal, RHAC had shown better performance than CAC as it gave low metal contents in AAS. The response surface methodology (RSM) was used to study the optimum process parameters that would maximise the efficiency of the process. There are two factors that were manipulated, which are the weight of adsorbent (A) and speed of mixing (B). For CAC, the optimum value of factors A was 4.00 g while the B was set to 524.89 rpm. Meanwhile, for RHAC, the optimum value of factors A was 2.29 g while the B was set to 4000 rpm. CAC has higher desirability with 0.83 compared to RHAC with 0.69.

KEYWORDS: Acid clay treatment; activated carbon; optimization; response surface methodology; used lubricating oil

INTRODUCTION

Lubricating oil (LO) is base oil mixed with additives to enhance their characteristics, which can be used to minimize wearing that is caused by physical friction [1]. During usage, the LO will undergo changes in terms of degradation, oxidation, and contamination, which make the lubricating oil ineffective for further application and need to be replaced [2]. Used lubricating oil (ULO) is a highly

hazardous waste that requires responsible management due to increasing quantities generated by automotive and industrial activities worldwide. It can cause a detrimental effect on the environment if it is not properly disposed of, handled, or treated [3,4]. Normally, ULO has high contaminants such as carbon residue, asphaltenic materials, heavy metals, water, and others [5]. Such pollutants can cause pollution to the environment to a large extent, where each volume can pollute not less than two hundred and fifty thousand volumes of water [6,7]. Developing countries have rapid urbanization and industrialization activity that has resulted in a large number of industrial wastes consisting of ULO. The percentage has been increasing throughout the years due to modernization and urbanization. It can be said that improper management of ULO can cause detrimental effects not just to the environment but also to humankind when it is not treated properly. Thus, in order to solve this problem, recovery of ULO can be one of the possible solutions [8-11]. Recovery of ULO has many advantages which include it is environmentally friendly, cost-effective and consumes lower energy in recycling.

Various treatment technologies are applied in order to recover and reclaim the ULO to its base oil form and remove contaminants [11-14]. Udonne [15] stated that acid clay method is the best method in recycling ULO. A comparative study had been conducted between different methods of recycling ULO. Acid- clay method using acetic acid is more effective compared to sulphuric acid in ULO recovery [16]. Hamawand *et al.* [16] concluded that acetic acid does not react chemically with the base oil compared to sulphuric acid, which reacts with base oil and might release sulphur dioxide to the atmosphere. However, the acid-clay method for the re-refining of ULO produces residual sludge which can pollute the soil and give low yield [17]. There are several research papers that use activated carbon (AC) in the treatment of the ULO [18,19]. According to a research conducted by Abdel-Jabbar *et al.* [5], they managed to recover the ULO by using various types of adsorbents such as date palm kernels powder, bentonite, and eggshell powder. The AC used in the treatment is a good material for the treatment of ULO, especially to reduce metal concentrations [18]. However, to date, the optimisation of the process parameters for ULO treatment by adsorption process using adsorbents is still lacking in much of the published literature.

Hence, the aim of this study was to recover oil from ULO and optimise the parameters to produce the high-quality base LO as well as to reduce the environmental impacts. In this study, there were two types of AC which are coconut AC (CAC) and rice husk AC (RHAC) used to recover the ULO. This study focused on the effectiveness of those ACs by characterizing the recovered oil and optimized the value for parameters in order to obtain the minimized value for both absorbances. The parameters such as weight of adsorbent and speed of mixing were optimized using the response surface methodology (RSM). Meanwhile, the responses that are being observed are the absorbance of fourier transform infrared spectroscopy (FTIR) and absorbance of ultraviolet-visible (UV-vis) spectroscopy.

MATERIALS AND METHODS

Materials

ULO samples (were collected from local car oil-change shops. The powdered CAC and RHAC had been obtained from Zhengzhou Zhongchuang Water Purification Material Co., Ltd, China. Glacial acetic acid (purity, 99.5%) for acid treatment was purchased from Sigma Aldrich. The recovered oil

was analysed through analytical characterizations, which are FTIR (Bruker INVENIO® R), UV-vis spectroscopy (Perkin Elmer LAMBDA™ 365) and atomic absorption spectrometry (AAS) (Hitachi Z-5000 Polarized Zeeman Flame/Graphite Furnace). Table 1 shows the physical characterization data for both ACs.

Table 1. Physical characterization data of powdered CAC and RHAC

Sl. no	Description	Unit	Detection result
1	Particle size	mesh	200
2	Iodine value	mg/g	700
3	Moisture	%	5
4	Ash content	%	5
5	Methylene blue	mg/g	90
6	Proportion	kg/m ²	500

Experimental procedure

Before undergoing acid clay treatment, it is important that moisture content be removed completely from the ULO. The ULO sample was heated up in the oven at 250°C for approximately 1 h [20]. After that, the oil was allowed to cool down to room temperature before proceeding to the next step, filtration. The dehydrated oil was then filtered using a vacuum pump to remove any debris or impurities from the oil. In the acid treatment, 1 ml of glacial acetic acid was added into 10 ml of filtered oil followed up by heating and stirring using the hot plate under room temperature for about 1 h [16]. After that, the mixture was allowed to settle down for 24 h at room condition. The last step in acid treatment was to undergo centrifugation for 1 h in order to separate base oil from any contaminants. After acid treatment, AC treatment took place and 15 ml of the treated oil was mixed with 1 g, 2.5 g and 4 g of the AC. The same step was done for both ACs. The mixture of the adsorbent and the oil were heated up to 250°C and centrifuged with different speeds of 500 rpm, 2300 rpm and 4000 rpm for 30 min [16]. The oil was filtered by using filter paper and the final oil recovered from the treatment was analysed.

FTIR analysis

FTIR analysis of the recovered oil was undergone in order to determine the functional groups. The range of FTIR used was in between 4000-400 cm⁻¹.

Concentration using UV-vis spectroscopy

UV-vis spectroscopy analysis of the recovered oil was undergone to determine concentration of oil sample. As the colour of treated LO remained dark, the absorbance of the treated EO was high as well. Treated oil samples (1 ml) were diluted with kerosene (10 ml) before being examined using a UV-vis spectrophotometer. Kerosene was selected because it is more suitable for mass spectrometric analysis [21].

Metal content analysis

Before the analysis, the recovered oil sample was heated to 60°C, stirred to ensure the homogeneity of the sample and was combined with ten volumes of kerosene (ratio 1:10) [22]. Metal concentrations were determined from the calibration curve obtained from standard solutions.

RSM modelling

RSM is known as a collection of mathematical and statistical techniques for empirical modelling. The main objective of RSM was to maximize the response that is influenced by various independent variables. The optimization was created using Design Expert 12 to evaluate the numerical accuracy and precision of the models developed. Performance evaluation apps are known as excellent indicators. In this study, a 3-level factorial design was applied. Other designs that are commonly used, for example Box-Behnken and central composite design (CCD) are usually used for more than two factors as the full factorial design needs more experimental runs than 3-level factorial. Before applying the RSM technique, it is necessary to select an experimental design to determine the courses that should be carried out within the experimental range being studied. There are two factors that were manipulated, which are the weight of adsorbent (A) and speed of mixing (B). The range of A was 1 g to 4 g for 15 ml of ULO while the range of B was 500 rpm to 4000 rpm [23]. Table 2 shows the model information used in RSM.

Table 2. Model information used in RSM

Factor	Units	Type	Coded low	Coded high
A	g	Numeric	-1 ↔ 1.00	1 ↔ 4.00
B	rpm	Numeric	-1 ↔ 500.00	1 ↔ 4000.00

RESULTS AND DISCUSSION

FTIR analysis

In this study, the virgin lubricating oil (VLO) was used as a reference to identify the effectiveness of the adsorption. Figure 1 shows the FTIR analysis of VLO and ULO.

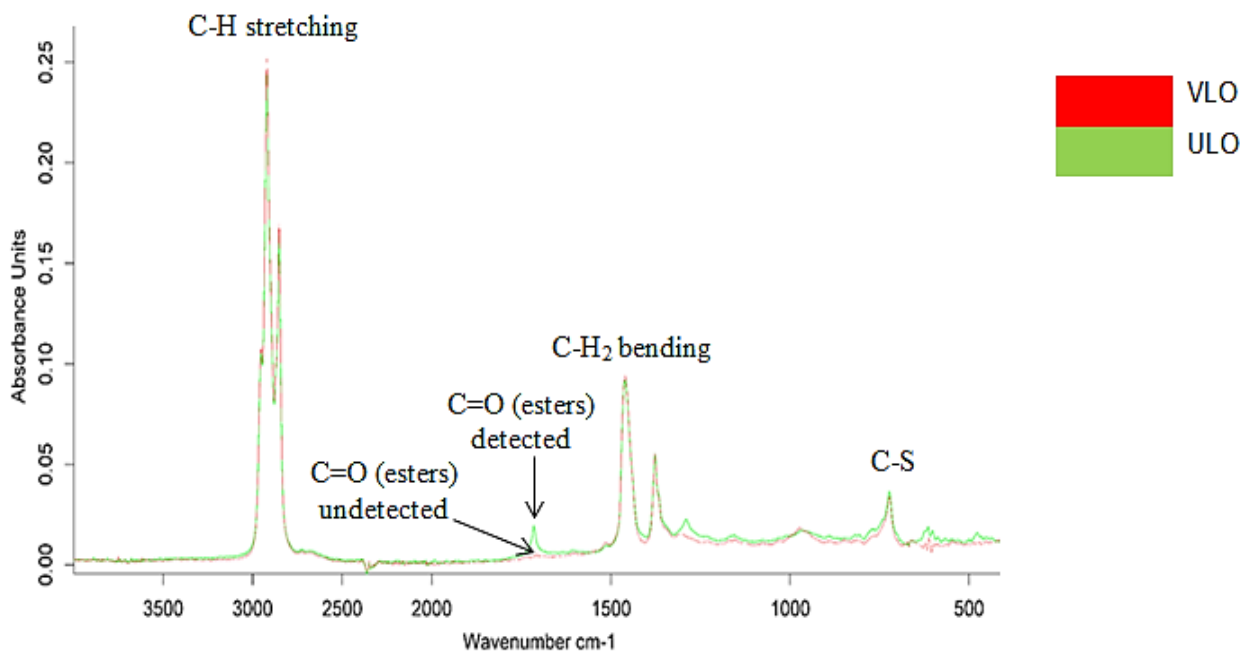


Figure 1. FTIR analysis of VLO and ULO

Table 3 shows the wavelenghts of components that were found in VLO and ULO

Table 3. Wavelengths of components that were found in VLO and ULO

Sample	Wavelength (cm ⁻¹)				
	C-H stretching	C-H ₂ bending	C=O (esters)	C-S	S=O stretching
VLO	2921.07 2852.46 1376.78	1460.13	UD	722.59	UD
ULO	2921.06 2852.47 1376.80	1460.35	1715.23	722.59	UD

Based on Figure 1 and Table 3, it was observed that the VLO contains C-H stretching with a wavelength at 2921.07 cm⁻¹, 2852.46 cm⁻¹ and 1376.78 cm⁻¹ whilst C-H₂ bending found at 1460.13 cm⁻¹ and C-S was found at at 722.59 cm⁻¹. According to Timur [24], the LOs consist of long chain hydrocarbons. Other components such as carbonyl groups which are caused by oxidation were undetected (UD). Meanwhile for ULO, it also contains C-H stretching with a wavelength at 2921.06 cm⁻¹, 2852.47 cm⁻¹ and 1376.80 cm⁻¹ whilst C-H₂ bending is found at 1460.35 cm⁻¹ and C-S group was found at at 722.59 cm⁻¹. However, the presence of carbonyl group at wavelength of 1715.23 cm⁻¹ with higher absorbance units indicated that the ULO was being contaminated due to the oxidation. Based on a study conducted by Honda T and Sasaki [25], the causes of lubricating oil contamination are roughly classified into two types: the contamination caused by solid particles and oil oxidation products.

After undergoing acid clay treatment using the two different types of AC, it had improved the properties of the ULO by removing the carbonyl compound that was originally present in the ULO. However, S=O group was found in a few samples of oil that had been treated. Figure 2 shows FTIR analysis of treated ULO using CAC (samples A-M).

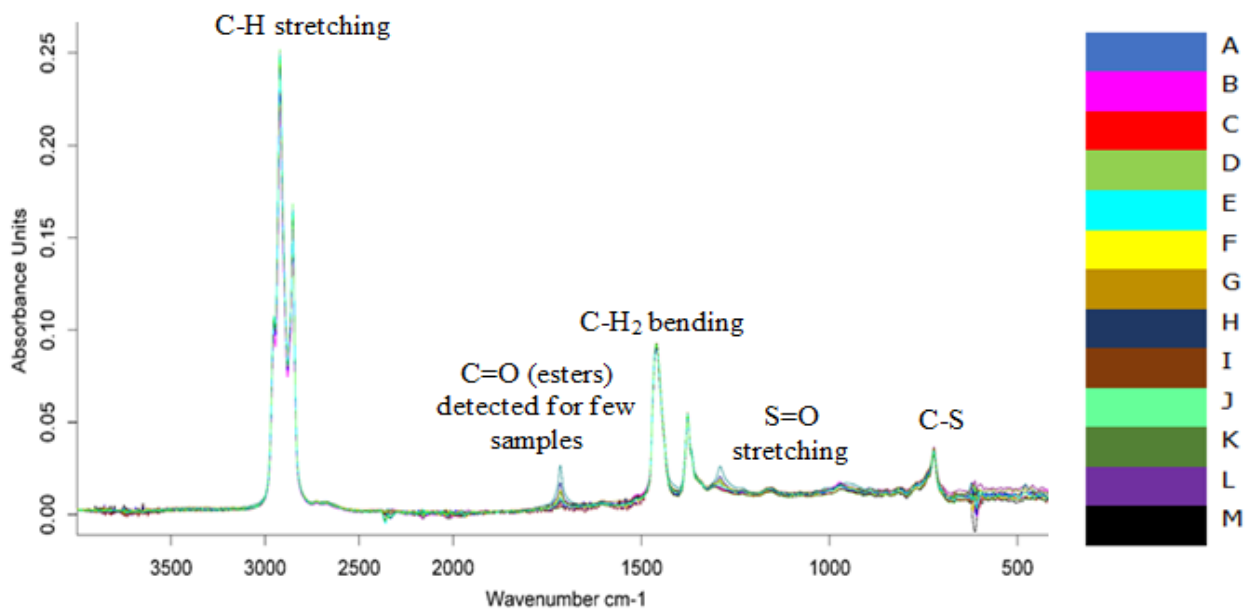


Figure 2. FTIR analysis of treated ULO using CAC

Table 4 shows wavelengths of components that were found in the treated ULO using CAC (samples A-M).

Table 4. Wavelengths of components that were found in the treated using CAC

Samples	Wavelength (cm ⁻¹)				
	C-H stretching	C-H ₂ bending	C=O (esters)	C-S	S=O stretching
A	2921.08				
	2852.45	1458.16	UD	722.29	UD
	1376.59				
B	2921.12				
	2852.48	1460.09	1715.23	722.69	1289.83
	1376.75				
C	2921.12				
	2852.47	1459.96	UD	722.23	UD
	1376.73				
D	2921.14				
	2852.50	1460.01	UD	722.37	UD
	1376.76				
E	2921.17				
	2852.49	1460.15	UD	722.25	UD
	1376.78				
F	2921.20				
	2852.51	1460.41	1714.94	721.98	UD
	1376.77				
G	2921.13				
	2852.47	1460.15	UD	722.20	UD
	1376.74				
H	2921.19				
	2852.51	1460.02	1715.29	722.19	1290.13
	1376.74				
I	2921.11				
	2852.50	1459.29	UD	722.13	UD
	1376.63				
J	2921.03				
	2852.41	1460.04	UD	722.07	UD
	1376.63				
K	2921.12				
	2852.47	1460.18	1715.36	722.18	1289.99
	1376.77				
L	2921.17				
	2852.52	1459.97	1715.27	721.85	1290.55
	1376.80				
M	2921.15				
	2852.48	1459.05	UD	722.35	UD
	1376.67				

For CAC, samples B, F, H, K, and L were indicated the presence of the carbonyl group at 1715.23 cm^{-1} , 1714.94 cm^{-1} , 1715.29 cm^{-1} , 1715.36 cm^{-1} and 1715.27 cm^{-1} , respectively. The presence of S=O was also found in samples B, H, K and L at 1289.83 cm^{-1} , 1290.13 cm^{-1} , 1289.98 cm^{-1} and 1290.55 cm^{-1} . Figure 3 shows FTIR analysis of treated ULO using RHAC (samples A1-M1).

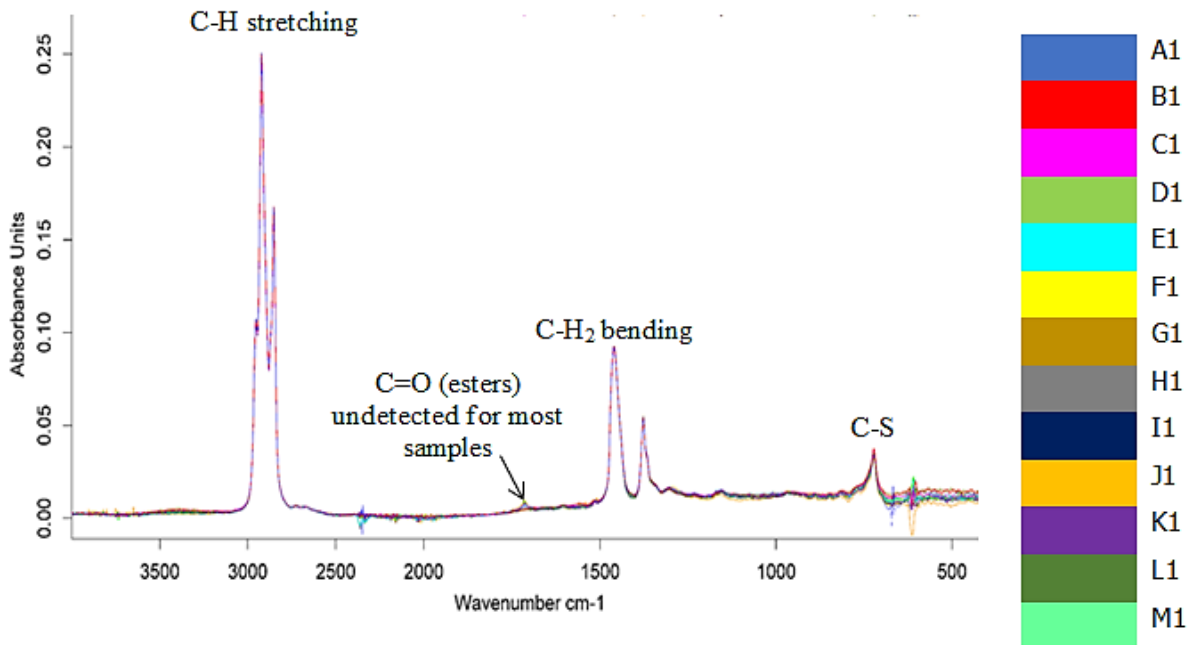


Figure 3. FTIR analysis of treated ULO using RHAC

Table 5 shows wavelengths of components that were found in the treated ULO using RHAC (samples A1-M1).

Table 5. Wavelengths of components that were found in the treated ULO using RHAC

Samples	Wavelength (cm^{-1})				
	C-H stretching	C-H ₂ bending	C=O (esters)	C-S	S=O stretching
A1	2921.18				
	2852.49	1460.08	UD	721.85	UD
	1376.73				
B1	2921.13				
	2852.47	1460.16	UD	722.04	UD
	1376.72				
C1	2921.16				
	2852.47	1460.24	UD	721.95	UD
	1376.74				
D1	2921.13				
	2852.51	1460.13	UD	722.03	UD
	1376.76			609.88	

E1	2921.16	1460.20	1715.88	722.27	UD
	2852.49			609.50	
	1376.75				
F1	2921.20	1460.19	UD	722.32	UD
	2852.48				
	1376.74				
G1	2921.11	1460.14	UD	721.80	UD
	2852.46				
	1376.73				
H1	2921.12	1460.10	UD	722.13	UD
	2852.48				
	1376.71				
I1	2921.17	1460.24	UD	722.09	UD
	2852.51			609.77	
	1376.74				
J1	2921.14	1460.33	UD	722.19	UD
	2852.48				
	1376.72				
K1	2921.05	1460.42	UD	722.23	UD
	2852.46				
	1376.75				
L1	2921.15	1460.45	UD	722.29	UD
	2852.46				
	1376.73				
M1	2921.14	1459.87	1715.90	722.48	UD
	2852.52				
	1376.72				

Based on Figure 3 and Table 5, for RHAC, samples E1 and M1 indicated the presence of the carbonyl group at wavelength of 1715.88 cm^{-1} and 1715.90 cm^{-1} , respectively. Meanwhile, the presence of S=O was not found in the samples.

UV-vis spectroscopy analysis

Table 6 shows the absorbance values of LO samples analysed by UV-vis spectroscopy. The VLO peak identified at 665.1 nm was used to analyse the absorbance. As on Table 6, at peak of 665.1 nm, the absorbance VLO was 0.023 whilst for ULO was 3.427. This shows that ULO has higher absorbance which means the quantity of light that passes is high due to the high concentration and the colour of the oil is darker. It also can be observed that all the samples that have been treated showed lower absorbance than untreated ULO. It means the adsorption process managed to improve the colour of the treated samples. For oil treated by CAC (samples A-M), the highest absorbance can be obtained in sample I with 2.957 while the lowest absorbance is in sample 0.603. Meanwhile for oil samples treated with RHAC (samples A1-M1), the highest absorbance can be obtained is 2.582 in sample K1 and the lowest absorbance is in sample C1 with 0.857.

Table 6. Absorbance analysed using UV-vis spectroscopy

		Peak = 665.1 nm	
Samples		Absorbance	
VLO		0.023	
ULO		3.427	
Oil treated using CAC		Oil treated using RHAC	
Samples	Absorbance	Samples	Absorbance
A	0.603	A1	1.269
B	1.644	B1	1.873
C	1.308	C1	0.857
D	1.596	D1	0.902
E	1.361	E1	1.044
F	1.738	F1	0.949
G	2.024	G1	2.284
H	1.235	H1	1.076
I	2.957	I1	1.951
J	2.656	J1	2.387
K	2.769	K1	2.582
L	0.976	L1	1.806
M	1.246	M1	1.193

AAS analysis

Table 7 shows the metal content found in the VLO, untreated ULO and ULO samples after being treated using CAC and RHAC. Table 7 shows that in the VLO, no metal content such as Pb, Cu and Fe was found, while for untreated ULO all of these metals were obtained. For oil samples treated using CAC, no Pb content was found, meaning the metal was fully absorbed by the ACs (Table 7). Meanwhile, for metal Cu, there was a decrease after being treated. Even samples D, I, and M showed no Cu content. For Fe, the metal content only showed a slight decrease after being treated. Only one sample E showed no Fe content. For oil samples treated using RHAC, metal content of Pb was fully absorbed after being treated (Table 7). Meanwhile, for metal Cu, it experienced a significant decrease after being treated. Samples B1, G1, I1 and J1 showed no metal content of Cu. For metal Fe, the metal content also showed a significant decrease after being treated.

Table 7. Metal content found in LO samples

Samples	Metal content (ppm)						
	Pb	Cu	Fe				
VLO	0.0000	0.0000	0.0000				
ULO	0.0121	0.3680	4.1623				
Oil treated using CAC			Oil treated using RHAC				
	Pb	Cu	Fe		Pb	Cu	Fe
A	0.0000	0.0954	0.2964	A1	0.0000	0.1174	1.1766

B	0.0000	0.1613	0.6338	B1	0.0000	0.0000	0.4431
C	0.0000	0.1503	2.1156	C1	0.0000	0.0132	1.0813
D	0.0000	0.0000	3.2600	D1	0.0000	0.0570	1.4261
E	0.0000	0.0845	0.0000	E1	0.0000	0.0680	1.4847
F	0.0000	0.0351	1.0739	F1	0.0000	0.0516	1.3600
G	0.0000	0.0077	2.5300	G1	0.0000	0.0000	0.8319
H	0.0000	0.1009	1.4114	H1	0.0000	0.0680	0.6045
I	0.0000	0.0000	3.1406	I1	0.0000	0.0000	0.6045
J	0.0000	0.0241	2.6931	J1	0.0000	0.0000	0.7365
K	0.0000	0.1448	3.0305	K1	0.0000	0.0516	1.0373
L	0.0000	0.1229	1.3820	L1	0.0000	0.0132	0.7952
M	0.0000	0.0000	2.4217	M1	0.0000	0.1174	1.2500

Optimization of experimental design by using RSM

The Table 8 and Table 9 represent the sets of experiments in the model run in Design Expert 12 for CAC and RHAC, respectively. Both the tables also show the responses obtained after experiments had been conducted.

Table 8. Set of experiments in the RSM model for CAC

Run	Factor 1 (A)	Factor 2 (B)	Response 1 (FTIR)	Response 2 (UV-vis spectroscopy)
1	4	500	0.02951	0.603
2	2.5	2300	0.02252	1.644
3	2.5	4000	0.0163	1.308
4	4	4000	0.01446	1.596
5	4	2300	0.01315	1.361
6	1	2300	0.01233	1.738
7	2.5	2300	0.01145	2.024
8	2.5	500	0.01110	1.235
9	2.5	2300	0.00199	2.957
10	2.5	2300	0.00198	2.656
11	1	4000	0.00099	2.769
12	1	500	0.00098	0.976
13	2.5	2300	0.00097	1.246

Table 9. Set of experiments in the RSM model for RHAC

Run	Factor 1 (A)	Factor 2 (B)	Response 1 (FTIR)	Response 2 (UV-vis spectroscopy)
1	4	500	0.00055	1.269
2	2.5	2300	0.0001	1.873
3	2.5	4000	0.00101	0.857
4	4	4000	0.00178	0.902
5	4	2300	0.00171	1.044
6	1	2300	0.00192	0.949
7	2.5	2300	0.0008	2.284
8	2.5	500	0.00092	1.076
9	2.5	2300	0.00043	1.951
10	2.5	2300	0.00041	2.387
11	1	4000	0.00048	1.582
12	1	500	0.00046	1.806
13	2.5	2300	0.00089	1.193

Optimization of experimental design using RSM for CAC

The statistical analysis of this experiment was dependent on the analysis of variance (ANOVA). The analysis was done by studying the p-value, R^2 and adjusted R^2 [26, 27]. The statistical analysis was tabulated based on the ANOVA variance analysis.

Effect of parameters on the absorbance of FTIR for CAC

After analysis had been conducted, the suggested modelling technique was a linear model for the absorbance of FTIR. After applying the developed model using the previously defined data, the following pre-model has been obtained. Equation (1) shows the final equation for absorbance of FTIR in terms of actual factors.

$$R = 0.031657 - 0.005704 \times A - 2.98713 \times 10^{-6} \times B \quad (1)$$

Where R represents absorbance of FTIR for CAC; A represents weight of adsorbent, g; B represents speed of mixing, rpm

Regression coefficients and ANOVA for the predicted response surface model shows in Table 10.

Table 10. ANOVA for the absorbance of FTIR for CAC

Source	Sum of Squares	Mean Square	F-value	p-value	
Model	0.0006	0.0003	7.93	0.0086	significant
A	0.0004	0.0004	11.55	0.0068	
B	0.0002	0.0002	4.31	0.0645	
Residual	0.0004	0.0000			
Lack of fit	0.0001	0.0000	0.4138	0.8398	not significant
Pure error	0.0002	0.0001			
Cor total	0.0010				

Standard deviation	0.0062	R^2	0.6134
Mean	0.0106	Adjusted R^2	0.5361
C.V. %	58.21	Predicted R^2	0.3831
	Adequate precision		9.3062

Based on Table 10, it was observed that the calculated model F-value of 7.93 (as it is desirable to have the biggest value) which implies the model is significant [21]. However, to specify that model terms are significant, p-value should be less than 0.05. p-value less than 0.05 indicate model terms are significant (Table 10). Behera *et al.* [28] stated that the larger the F-value and the lower the p-value implies that the model is significant. There is only 0.86% chance that an F-value this large could occur due to noise. In this case only factor A is regarded as a significant model term. The lack of fit F-value of 0.4138 implies that the lack of fit is not significant relative to the pure error. There is an 83.98% chance that a Lack of Fit F-value this large could occur due to noise. Non-significant lack of fit is good as the model needs to be fitted. The ‘Predicted R^2 ’ of 0.3831 is in practical agreement with the ‘Adjusted R^2 ’ of 0.5361 with a difference of less than 0.2. Adequate precision measures the signal to noise ratio. A ratio greater than 4 is desirable. The ratio of 9.306 indicates an adequate signal. This model can be used to navigate the design space. Besides, the lower standard deviation portrays that a good model that gives a good value between predicted and actual value of the response [28]. Figure 4 shows the interactions between each component in a three-dimensional group based on ANOVA.

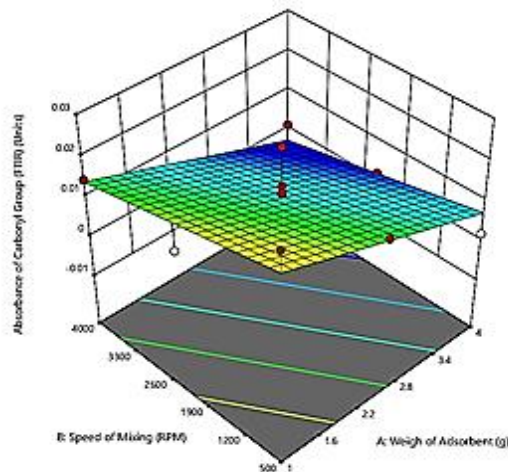


Figure 4. Variations in output experimental design with factors A and

Based on Figure 4, it illustrates the factors that affect the absorbance of FTIR for CAC. For factor A, as it is increased, the absorbance of the FTIR decreases. Meanwhile for factor B, the pattern was the same with factor A. Thus, it was found that with higher weight of adsorbent and speed of mixing, the absorbance of FTIR can be decreased.

Effect of parameters on the absorbance in UV-vis spectroscopy for CAC

Equation 2 shows the final equation for the absorbance in UV-vis spectroscopy in terms of actual factors

$$S = 1.60482 - 0.213667 \times A + 0.000277 \times B \quad (2)$$

Where S represents absorbance of UV-vis spectroscopy; A represents weight of adsorbent, g and B represents speed of mixing, rpm

Regression coefficients and ANOVA for the predicted response surface model shows in Table 11.

Table 11. ANOVA for the absorbance in UV-vis spectroscopy for CAC

Source	Sum of squares	Mean square	F-value	p-value	
Model	2.03	1.01	2.44	0.1371	not significant
A	0.6163	0.6163	1.48	0.2510	
B	1.41	1.41	3.39	0.0952	
Residual	4.15	0.4150			
Lack of fit	2.16	0.3607	0.7262	0.6548	not significant
Pure error	1.99	0.4966			
Cor total			6.18		
Standard deviation	0.6442			R^2	0.3279
Mean	1.70			Adjusted R^2	0.1935
C.V. %	37.87			Predicted R^2	-0.0121
	Adequate precision				5.2021

Table 11 shows that the F-value and p-value are 2.44 and 0.1371, respectively. These values clearly indicated that the model is not significant. There is a 13.71% chance that an F-value this large could occur due to noise. The lack of fit F-value of 0.7262 implies that this value is not significant relative to the pure error. The negative ‘Predicted R^2 ’ implies that the overall mean may be a better predictor of the response than the current model. In some cases, a higher order model may also predict better. Adequate precision was 5.2021 which indicate an adequate signal. Since it is higher than 4, thus this model can be used to navigate the design space. Figure 5 shows the interactions between each component in a three-dimensional group based on ANOVA.

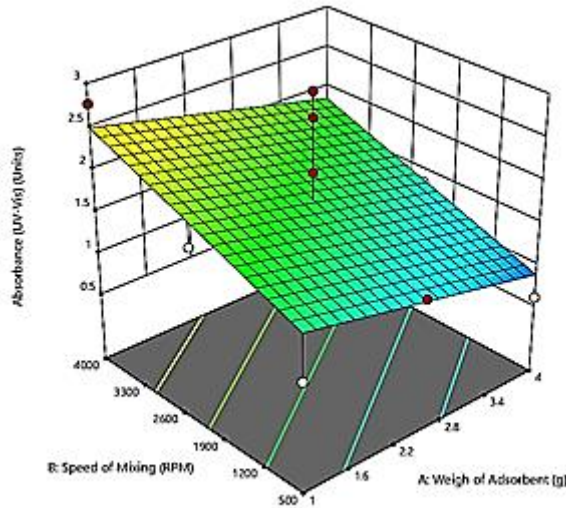


Figure 5. Variations in output experimental design with factors A and B

Based on Figure 5, it illustrates the factors that affect the absorbance of UV-vis spectroscopy. For factor A, as it is increased, the absorbance decreases. However, for factor Y, the pattern is not the same with factor A as the speed of mixing increases, the absorbance significantly increases. Thus, it can be concluded that with a higher weight of adsorbent and with lower speed of mixing, the absorbance in UV-vis spectroscopy can be decreased. According to Hussanin and Kamakar [29], the absorbance should be lower as the concentration of LO decreases, the absorbance should be decreased indicating that the oil is less deteriorated.

Effect of parameters on the absorbance of FTIR for RHAC

Equation 3 shows the final equation for absorbance of FTIR in terms of actual factors

$$R = 0.001990 - 0.001450 \times A + 2.08561 \times 10^{-7} \times B + 1.1356 \times 10^{-7} \times A \times B + 0.000265 \times A^2 - 8.1079 \times 10^{-11} \times B^2 \tag{3}$$

Regression coefficients and ANOVA for the predicted response surface model shows in Table 12.

Table 12. ANOVA for the absorbance of FTIR for RHAC

Source	Sum of squares	Mean square	F-value	p-value	
Model	1.869E-06	3.738E-07	1.18	0.4047	not significant
A	2.254E-07	2.254E-07	0.7127	0.4265	
B	2.993E-07	2.993E-07	0.9463	0.3631	
Residual	2.214E-06	3.162E-07			
Lack of Fit	1.802E-06	6.007E-07	5.84	0.0607	not significant
Pure Error	4.117E-07	1.029E-07			
Cor Total	4.083E-06				

Standard deviation	0.0006	R^2	0.4578
Mean	0.0009	Adjusted R^2	0.0705
C.V. %	63.79	Predicted R^2	-2.5141
	Adequate precision		4.0155

Table 12 shows that the F-value and p-value are 1.18 and 0.4047, respectively. These values clearly indicated that the model is not significant. There is a 40.47% chance that an F-value this large could occur due to noise. The lack of fit F-value of 5.84 implies that there is a 6.07% chance that a lack of fit F-value this large could occur due to noise. The negative ‘Predicted R^2 ’ implies that the overall mean may be a better predictor of the response than the current model. In some cases, a higher order model may also predict better. The ratio of ‘Adequate precision’ is 4.0155 which imply an adequate signal. Since the ratio is greater than 4, thus this model can be used to navigate the design space. Figure 6 shows the interactions between each component in a three-dimensional group based on ANOVA

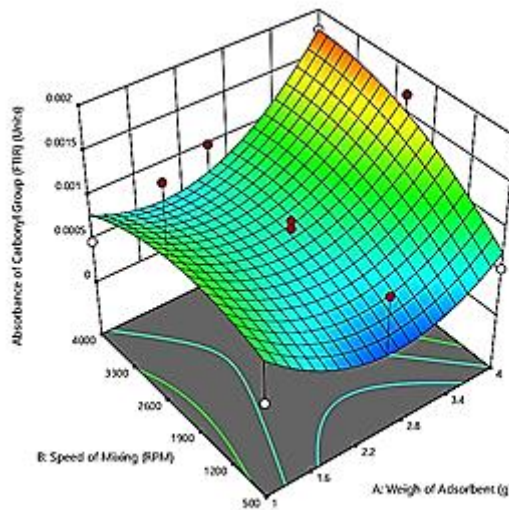


Figure 6. Variations in output experimental design with factors A and B

Based on Figure 6, it illustrates the factors that affect the absorbance of FTIR. For factor A, as it is increased, the absorbance of the FTIR decreases but only up to 2.5 g weight of adsorbent and then it increases back. Meanwhile for factor B, the pattern is vice versa with factor A whereas the speed of mixing increases, the absorbance of the FTIR also increases up until 2300 rpm and then it shows slightly decreases as the speed of mixing increases. Thus, it has found that there is a certain point that needs to be chosen in order to decrease the absorbance of the FTIR.

Effect of parameters on the absorbance of UV-vis spectroscopy for RHAC

Equation 4 shows the final equation the absorbance of UV-vis spectroscopy in terms of actual factors

$$S = 1.80555 - 0.124667 \times A - 0.000076 \times B \quad (4)$$

Regression coefficients and ANOVA for the predicted response surface model are shown in Table 13.

Table 13. ANOVA the absorbance of UV-vis spectroscopy for RHAC

Source	Sum of squares	Mean square	F-value	p-value	
Model	0.3158	0.1579	1.14	0.3569	not significant
A	0.2098	0.2098	1.52	0.2458	
B	0.1060	0.1060	0.7680	0.4014	
Residual	1.38	0.1380			
Lack of Fit	0.8908	0.1485	1.21	0.4449	not significant
Pure Error	0.4891	0.1223			
Cor Total			1.70		

Standard deviation	0.3715		R^2	0.1862
Mean	1.32		Adjusted R^2	0.0235
C.V. %	28.12		Predicted R^2	-0.2281
			Adequate precision	3.5850

Table 13 shows that the F-value and p-value are 1.14 and 0.3569, respectively. These values clearly indicated that the model is not significant. There is a 35.69% chance that an F-value this large could occur due to the noise. The lack of fit F-value of 1.21 implies the lack of fit is not significant relative to the pure error. There is a 44.49% chance that a lack of fit F-value this large could occur due to noise. The negative ‘Predicted R^2 ’ implies that the overall mean may be a better predictor of the response than the current model. In some cases, a higher order model may also predict better. The ratio of ‘Adequate precision’ is 3.5850 which implies an inadequate signal. Since the ratio is not greater than 4, this model should not be used to navigate the design space. Figure 7 shows the interactions between each component in a three-dimensional group based on ANOVA

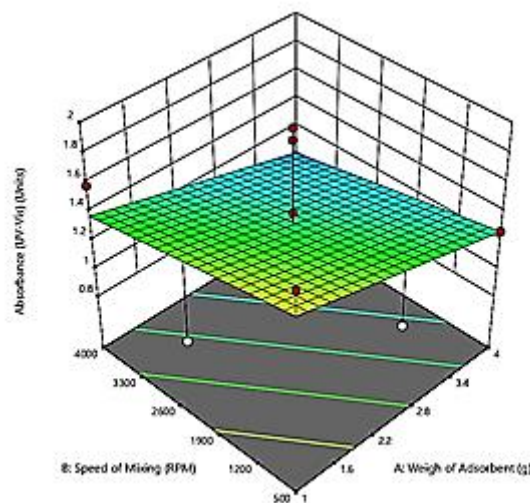


Figure 7. Variations in output experimental design with factors A and B

Based on Figure 7, it illustrates the factors that affect the absorbance of UV-vis spectroscopy. For factor A, as it is increased, the absorbance slightly decreases. Meanwhile for factor B, the pattern is the same with factor A whereas the factor B increases, the absorbance decreases. Thus, it can be concluded that with higher weight of adsorbent and speed of mixing, the absorbance in UV-vis spectroscopy can be decreased.

Comparison of optimization between CAC and RHAC

In this model the objective of optimization was to determine the best operating parameters that can be used to decrease both of the absorbance values of the ULO. Table 14 shows the comparison of optimization value of the factors between CAC and RHAC. Numerical method was conducted in order to determine optimum operating parameters. The goal for absorbance of FTIR and absorbance in UV-vis spectroscopy was being minimised as the values to be lowered. For CAC, the optimum value of factors A was 4.00 g while B was set to 524.89 rpm. Meanwhile, for RHAC, the optimum value of factors A was 2.29 g while B was set to 4000 rpm.

Table 14. Comparison of optimization value of the factors between CAC and RHAC

	CAC	RHAC
Name	Optimization value	Optimization value
A	4.00	2.29
B	524.89	4000
Absorbance of FTIR	0.05	0.01
Absorbance of UV-vis spectroscopy	0.90	1.22
Desirability	0.83	0.69

As Table 14 shows, RHAC produced the lowest value for absorbance of carbonyl group while CAC produced the lowest value of absorbance in UV-vis spectroscopy. CAC has higher desirability with 0.83 compared to RHAC with 0.69.

CONCLUSION

In conclusion, acid-clay treatment was proven in treating and improving the properties of ULO. The ULO could be best recovered with acid-clay treatment using the AC, as it is able to improve the quality of the ULO which is comparable with VLO. In terms of metal removal, RHAC had shown better performance than CAC as it gave low metal contents in AAS. This study also optimized the value for parameters in order to obtain the minimized value for both absorbances. For CAC, the optimum value of the factors is that A was 4.00 g while B was set to 524.89 RPM. Meanwhile, for RHAC, for factors A and B were 2.29 and 4000 rpm, respectively. CAC has higher desirability with 0.83 compared to RHAC with 0.69.

ACKNOWLEDGEMENTS

The authors pay their sincere gratitude to Universiti Malaysia Sabah (UMS) for providing necessary research facilities to accomplish this study.

REFERENCES

- Moura, L. G. M., Assunção Filho, J. L. and Ramos, A. C. S. (2010) Recovery of used lubricant oils through adsorption of residues on solid surfaces. *Braz. J. Petroleum Gas*, **4(3)**, 91–102.
- Josiah, P. N. and Ikiensikimama, S. S. (2010) Effect of desludging and adsorption ratios on recovery of low pour fuel oil (LPFO) from spent engine oil. *Chem. Eng. Res. Bull.*, **14(1)**, 25–28.
- Osman, D. I., Attia, S. K. and Taman, A. R. (2018) Recycling of used engine oil by different solvent. *Egypt. J. Pet.*, **27(2)**, 221–225.
- Diphare, M., Muzenda, E., Pilusa, T. J. and Mollagee, M. (2013) A comparison of waste lubricating oil treatment techniques. 2nd International Conference on Environment, Agriculture and Food Sciences, (ICEAFS'2013), Kuala Lumpur, Malaysia, 106–109.
- Abdel-Jabbar, N. M., Al Zubaidi, E. A. H. and Mehrvar, M. (2010) Waste lubricating oil treatment by adsorption process using different adsorbents. *Int. J. Chem. Biol. Sci.*, **3(2)**, 70–73.
- Udonne, J. D. and Bakare, O. A. (2013) Recycling of used lubricating oil using three samples of acids and clay as a method of treatment. *Inter. Arch. App. Sci.*, **4(2)**, 8–14.
- Rahman, M. M., Siddiquee, T. A., Samdani, S. and Kabir, K. B. (2008) Effect of operating variables on regeneration of base-oil from waste oil by conventional acid-clay method. *Chem. Eng. Res. Bull.*, **12**, 24–27.
- Anisuzzaman, S. M., Abang, S., Krishnaiah, D. and Azlan, N. A. (2019) Removal of used motor oil from water body using modified commercial activated carbon. *Malays. J. Chem.c* **21(1)**, 36–46.
- Aljabiri, N. A. (2018) A comparative study of recycling used lubricating oils using various methods. *J. Sci. Eng.*, **5(9)**, 168–177.
- Shaikh, R. and Mahanwar, P. (2018) Reclamation of used engine oil using polymeric flocculants. *Int. J. Chem. Sci.*, **16(2)**, 1–14.
- Omolara, A. M., Olurotimi, A. D., Olatunji, G. O. (2015) Regeneration of used lubricating engine oil by solvent extraction process. *Int. J. Energ. Env. Res.*, **3(1)**, 1–12.
- Kamal, A. and Khan, F. (2009) Effect of extraction and adsorption on refining of used lubricating oil. *Oil Gas Sci. Technol. - Rev. IFP*, **64(2)**, 191–197.
- Rincon, J., Cañizares, P. and García M. T. (2007) Regeneration of used lubricant oil by ethane extraction. *J Supercrit. Fluid.*, **39(3)**, 315–322.
- Hamad. A., Al-Zubaidy, E., Fayed, M. E. (2005) Used lubricating oil recycling using hydrocarbon solvent. *J Environ Manage.*, **74(2)**, 153–159.

- Udonne, J. D. (2011) A comparative study of recycling of used lubrication oils using distillation, acid and activated charcoal with clay methods. *J. Petroleum Gas Eng.*, **2(2)**, 12–19.
- Hamawand, I., Yusaf, T. and Rafat, S. (2013) Recycling of waste engine oils using a new washing agent, *Energies*, **6(2)**, 1023–1049.
- Shakirullah M., Ahmad I., Khan M. A., Ishaq M., Rehman H. and Saeed, M. (2006) Spent lubricating oil residues as new precursors for carbon. *Fuller. Nanotub. Car. N.*, **14(1)**, 39–48.
- Riyanto, T. A. A. and Juliantydwaji, D. P. (2018) The effect of treatment with activated carbon on the metal content in reuse of lubricating oil waste. *MATEC Web of Conferences*, **154 (01018)**, 1-5.
- Bhaskar, T., Uddin, A., Muto, A., Sakata, Y., Omura, Y., Kimura, K. and Kawakami, Y. (2004) Recycling of waste lubricant oil into chemical feedstock or fuel oil over supported iron oxide catalysts. *Fuel*, **83(1)**, 9–15.
- Emam, E. A. and Shoaib, A. M. (2012) Re-refining of used lube oil , II- by solvent/clay and acid/clay-percolation processes. *ARPJ. Eng. Appl. Sci.*, **2(11)**, 1034–1041.
- Osman H. (2019) Model Prediction and optimization of waste lube oil treated with natural clay. *Processes*, **7(10)**, 729–743.
- Mekonnen, H. A. (2014) Recycling of used lubricating oil using acid-clay treatment process, M. Sc. thesis, Addis Ababa University, Addis Ababa Institute of Technology (AAiT), 1–71.
- Oladimeji, T. E., Sonibare, J. A., Omoleye, J. A., Adegbola, A. A. and Okagbue, H. I. (2018) Data on the treatment of used lubricating oil from two different sources using solvent extraction and adsorption. *Data Brief*, **19**, 2240–2252.
- Timur A. (2017) Reclamation of used lubricating oils using magnetic nanoparticles and caustic soda; M. Sc. thesis; Department of materials science and engineering, Graduate school of engineering and science, Bilkent university; 1–81.
- Honda T and Sasaki A. (2018) Development of a turbine oil contamination diagnosis method using colorimetric analysis of membrane patches. *J. Adv. Mech. Des. Syst. Manuf.*, **12(4)** 1–8.
- Bono, A., Krishnaiah, D. and Rajin, M. (2008) Products and process optimization using response surface methodology, Universiti Malaysia Sabah Press, Kota Kinabalu, Sabah, Malaysia.
- Bono, A., Anisuzzaman, S. M. and Ding, O. W. (2014) Effect of process conditions on the gel viscosity and gel strength of semi-refined carrageenan (SRC) produced from seaweed (*Kappaphycus alvarezii*). *J King Saud Univ Eng Sci.*, **26(1)**, 3–9.
- Behera, S. K., Meena, H., Chakraborty, S. and Meikap, B. C. (2018) Application of response surface methodology (RSM) for optimization of leaching parameters for ash reduction from low-grade coal. *Int. J. Min. Sci. Technol.*, **28(4)**, 621–629.
- Hussain, K. and Karmakar, S. (2014) Condition assessment of transformer oil using UV-Visible spectroscopy; Power Systems Conference (NPSC), Eighteenth National, IEEE, 1–5.